

## Validation of an AACSR conductor with trapezoidal wires for a river crossing

P. VAN DYKE<sup>1</sup>, S. PRUD'HOMME<sup>2</sup>, J. PARADIS<sup>1</sup>

<sup>1</sup>Institut de Recherche d'Hydro-Québec    <sup>2</sup>Hydro-Québec  
Canada

### SUMMARY

The conductor of the St. Lawrence River crossing of a 230-kV line on the TransÉnergie network will be replaced to ensure its long-term operability. This crossing also currently limits the transit capacity of the line. To replace the current conductor, line design engineers proposed using a trapezoidal AACSR conductor to increase the conductor's aluminum section without changing its outer diameter. This solution makes it possible to increase the transit capacity of the line without increasing the climatic loads from ice and wind.

The span has a length of 1.46 km, and the mechanical tension on the conductor is very high, i.e., 230 kN, which corresponds to a line parameter  $H/w$  (mechanical tension over the linear weight of the conductor) of 6350 m. Such a high parameter increases the severity of wind vibrations that can lead to fatigue and conductor breakage, since it far exceeds the safe tension recommended by CIGRE for a single conductor with dampers [CIGRE TB 273, 2005]. In addition, the conductor is held in dead-end joints at each end of the span and there is no fatigue data available for such a conductor configuration. To ensure compliance with the conductor's endurance limit, a study was carried out on the conductor to determine its fatigue properties and internal damping and validate the planned damping system.

The endurance limit of the conductor in the dead-end joint was determined using the IEC 62568 standard and adapting it for a case where the conductor is retained by a dead-end joint.

The paper presents the test set-up used for the fatigue tests as well as the first results obtained. The tests were made by controlling the relative displacement ( $Y_b$ ) of the conductor at the outlet of the dead-end joint. Contrary to a standard set-up in a suspension clamp, the frequency times the antinode displacement  $fY_{\max}$  and the relative displacement  $Y_b$  of the conductor at the outlet of the dead-end joint are not directly proportional and depend on the excited vibration mode.

Aeolian vibration dampers with preformed rod attachments will be used to maximize the conductor's tolerance to vibration in the damper clamp and prevent problems of bolts loosening and dampers slipping along the conductor.

### KEYWORDS

Endurance limit, fatigue, river crossing, AACSR, compact conductor

**INTRODUCTION**

The conductor of the St. Lawrence River crossing of a 230-kV line built in 1958 on the TransÉnergie network will be replaced to ensure its long-term operability. The crossing consists of three single conductors and there is no ground wire. The length of the crossing is 1462 m and the lengths of the adjacent spans are 337 m on the North-West side and 368 m on the South-East side. The terrain is relatively flat on both riverbanks, and the crossing’s suspension towers are 120 m high while the adjacent anchor towers are 18 m high.

This crossing also currently limits the transit capacity of the line. To replace the current conductor, line design engineers therefore proposed using a trapezoidal wire AACSR conductor (TRA3RTW8) to increase the conductor’s aluminum section without changing its outer diameter. This solution makes it possible to increase the transit capacity of the line without increasing the climatic loads from ice and wind. Figure 1 shows the current conductor cross-section (18/61, A1/S3A, rated tensile strength (RTS) = 598 kN, m = 4.03 kg/m) and that of the replacement conductor TRA3RTW8 (A4/S3A, stranding 30/37, RTS = 518 kN, m = 3.7 kg/m).

The current conductor is anchored to the suspension towers at each end of the crossing as shown in Figure 2 and the same approach will be used for the replacement conductor. The dead-end joint of the replacement conductor is shown in Figure 3 as well as a section of the dead-end joint compressed on the conductor.

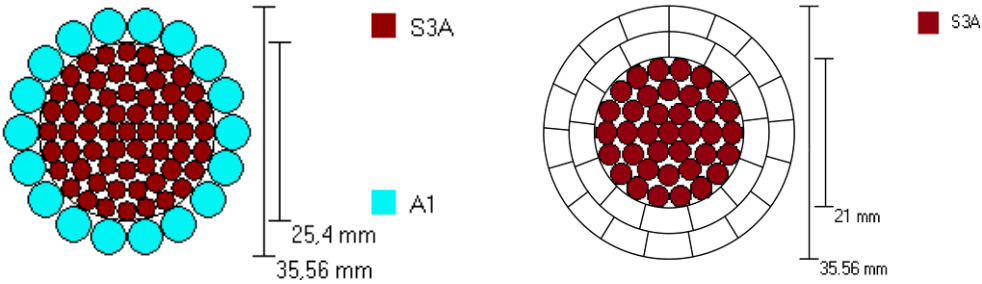


**Figure 1: Current conductor on the left and replacement conductor TRA3RTW8 on the right**

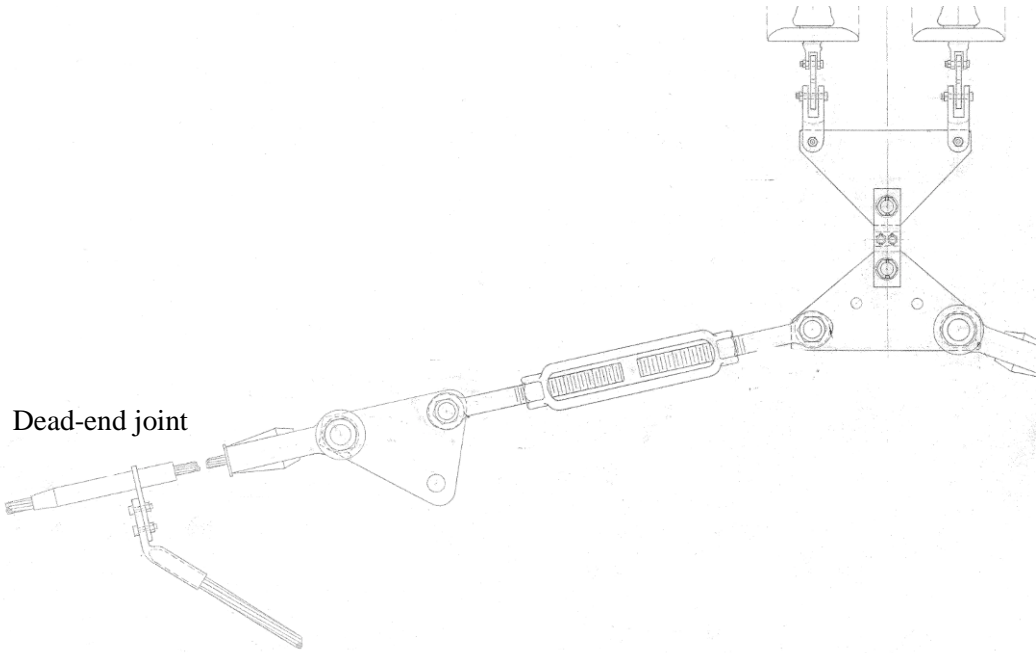


**Figure 2: Dead-end joint of the conductor at the suspension tower in the current river crossing**

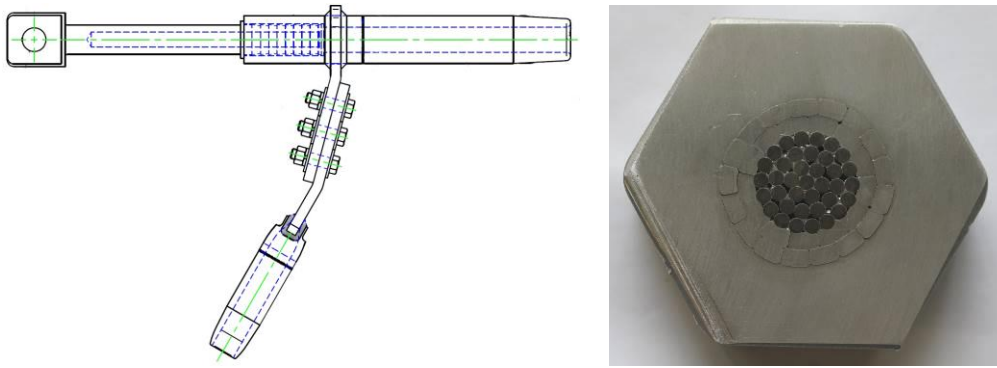


**Figure 3: TRA3RTW8 conductor dead-end joint and cut that shows the joint compressed on the conductor**

The mechanical tension of the TRA3RTW8 conductor will be very high, i.e., 230 kN, which corresponds to a line parameter H/w (mechanical tension over the linear weight of the conductor) of 6350 m. This tension is set for a temperature of  $-15^{\circ}\text{C}$ , which is the average temperature of the month of January at this location. Such a high parameter increases the severity of wind vibrations that can lead to fatigue and conductor breakage, since it far exceeds the safe tension recommended by CIGRE for a single conductor with dampers [CIGRE TB 273, 2005]. Consequently, to ensure compliance with the conductor's acceptable vibration criteria, a study was performed to determine its fatigue properties and internal damping and validate the damping system that will be installed.

The fatigue endurance limit for this AACSR conductor must be determined experimentally because the combination of the following characteristics means that there is no available data to estimate the conductor's endurance limit:

- Aluminum alloy wire conductor
- Trapezoidal wire conductor
- Conductor retained by dead-end joints rather than being supported in a suspension clamp
- Very high conductor' H/w setting of 6350 m

The tests to determine the endurance limit of the TRA3RTW8 conductor were made using the IEC 62568 [2015] standard and adapting it for a case where the conductor is held by dead-end joint. The next section presents the test set-up used for the fatigue tests as well as the first results obtained.

Aeolian vibration dampers with preformed rod attachments will be used to maximize the conductor's tolerance to vibration in the damper clamp and prevent problems of bolts loosening and dampers slipping along the conductor. Validation of the effectiveness of the damping system will be published in a subsequent paper.

## **TEST SET-UP**

### **Test bench**

IEC 62568 [2015] was written to ensure that fatigue tests on specific conductor/clamp systems reproduce field load conditions as accurately as possible. The standard therefore specifies that the clamp must be fixed to prevent movement and the test bench must reproduce the exit angle of the conductor at the clamp. The Hydro-Québec Research Institute already has six test benches that were designed according to this standard, however, for this study, new benches had to be designed because rather than being supported in suspension clamps, the conductor is held in dead-end joints at each end of the test span. In addition, the mechanical tension of the conductor was too high for our existing benches.

Four test benches were built this way. For each bench, the dead-end joint is retained by its eyelet at one end (Figure 4 and Figure 5) and the conductor is excited with a shaker at the other end (Figure 6). The four benches are installed in series (Figure 7) and the conductor is clamped on a structure anchored to the ground between each bench to minimize the amplitude of the vibrations transmitted between the benches.

The severity of the vibrations is quantified using a relative displacement sensor transducer on the dead-end joint which measures the relative displacement of the conductor at 89 mm from the last point of contact between the conductor and the dead-end joint (Figure 4 and Figure 5).

The length of each test bench, measured from the eyelet of the dead-end joint to the clamp at the other end near the shaker varies between 12.06 and 12.77 m. The TRA3RTW8 conductor was installed at a mechanical tension of 230 kN.



**Figure 4: Dead-end joint of span 1**



**Figure 6: Test span 1**



**Figure 5: Dead-end joint of span 3**



**Figure 7: View of the four test spans**

### **Relative displacement according to the excited mode**

In order to minimize the duration of the tests, they were performed in mode 6, which produces a frequency that varies between 59 and 60 Hz for the different test spans, where 60 Hz is the maximum frequency allowed for these tests according to the IEC 62568 [2015]. For this mode, the loop length of the stationary vibration is 2.12 m except for the first loop, where the dead-end joint is located, which is 1.39 m long. The distance between the center of the eyelet of the dead-end joint and its other end is 0.92 m, or 66% of the length of the first loop of vibration.

For standard tests in a fixed clamp, the relative displacement  $Y_b$  at the output of the clamp is proportional to the frequency multiplied by the antinode amplitude of the conductor  $fY_{\max}$ . With the

test set-up used here, this is no longer the case because the relative displacement will be influenced by the position of the anchor sleeve in the excited wavelength. The relative displacement of the conductor at the outlet of the dead-end joint was measured at different vibration modes of the test span before each test by exciting the conductor at an amplitude  $fY_{max}$  of 50 mm/s. The results are shown in Figure 8 for modes 1 to 10 for test 1 and for modes 4 to 6 for tests 2 to 5. Note that the relative displacement gradually increases to mode 5 and decreases thereafter. The relative displacement is at its maximum when the outlet of the dead-end joint is located near the center of the vibration loop. The tests were therefore performed by controlling the relative displacement ( $Y_b$ ) of the conductor at the outlet of the dead-end joint.

The relative displacement was measured for  $fY_{max}$  amplitudes of 50, 100 and 150 mm/s in mode 6 for two different tests. For a given excitation mode, there is no non-linearity as a function of the amplitude for this excitation range and  $Y_b$  is directly proportional to  $fY_{max}$  as shown in Figure 9.

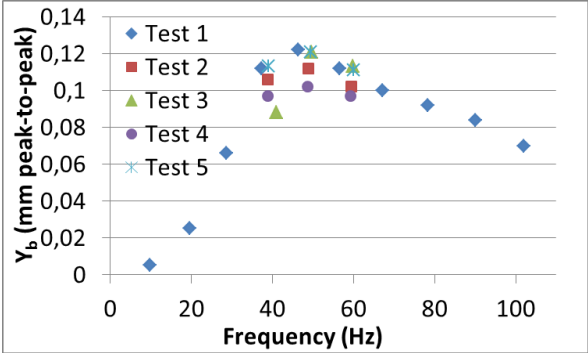


**Figure 8: Relative displacement as a function of the excited mode**

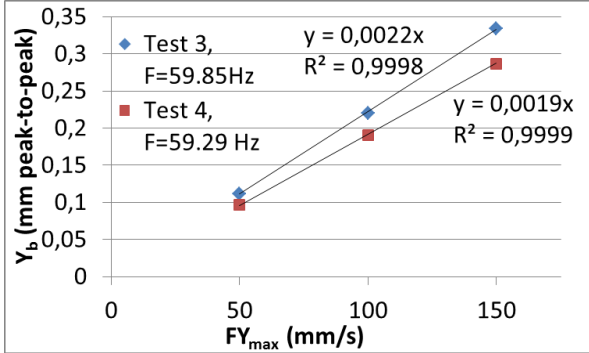


**Figure 9: Relative displacement as a function of the amplitude  $fY_{max}$**

**TEST RESULTS**

Eight fatigue tests have been completed so far on the TRA3RTW8 conductor with the following relative displacements:  $Y_b = 0.6, 0.51, 0.4, 0.31, 0.205, 0.153, 0.151$  and  $0.158$  mm peak-to-peak. The tests were stopped after three breaks, except the tests with  $Y_b = 0.151$  and  $0.205$  mm peak-to-peak for which only two breakages were obtained. Four tests are currently under way with 138 Mcycles completed without breakage at an amplitude of 0.1 mm peak-to-peak on three tests and 61 Mcycles completed without breakage at an amplitude of 0.125 mm peak-to-peak on one test. The relative displacement  $Y_b$  of the conductor at the outlet of the dead-end joint, the amplitude  $fY_{max}$  at the vibration antinode and the signals of two conductor wire break detectors are measured continuously during each test.

Figure 10 shows an example of fretting fatigue breakage of wires on the outer layer of the conductor during a test. The number of cycles before failure (SN curve) is illustrated in Figure 11 in terms of  $Y_b$  and in Figure 12 in terms of  $\sigma(Y_b)$  [EPRI, 2009] where they are compared with a combination of the results previously obtained at GREMCA [2002] and IREQ [Paradis and Van Dyke, 2019] on a standard ACSR Crow conductor (ACSR 54/7) at a mechanical tension of 29 kN (25% RTS) in a metal-metal type clamp (model Slacan 62065) (Figure 13). Although data is still missing to establish the TRA3RTW8 conductor’s endurance limit, it is clear that its endurance limit will be much lower than that of an ACSR. Such a result was anticipated because it is already known that the following three factors reduce the endurance limit [EPRI, 2009].

- The use of aluminum alloy
- Very high mechanical tension

- The use of dead-end joints that have more severe exit angles than a suspension clamp.

Although a decrease in the endurance limit was anticipated, it was more severe than expected. Table 1 provides the ratio of the number of cycles before failure for the two conductors. The number of cycles that the Crow conductor can accumulate before breaking compared to a TRA3RTW8 increases as the amplitude decreases. However, it is important to understand that even if the endurance limit expressed as a function of  $Y_b$  is much lower for the TRA3RTW8 in a dead-end joint, this does not mean that the conductor will be problematic. Indeed, as shown above in this paper, the relative displacement is at its maximum when the end of the joint is close to the vibration antinode, while the relative displacement is less severe for other frequencies. It will therefore be necessary to ensure that the chosen damping system adequately protects the conductor over the entire range of frequencies of interest and in particular at frequencies for which the end of the sleeve is close to the vibration belly.



**Figure 10: Trapezoidal wire breakage due to fretting fatigue on the outer layer of the conductor at the outlet of the dead-end joint**

**Table 1: Ratio of the number of cycles before break between the two S-N curves for different values of  $\sigma_a(Y_b)$**

$\sigma_a(Y_b)$ (MPa)	Ratio between S-N curves (Crow/TRA3RTW8)
20	6
13	59

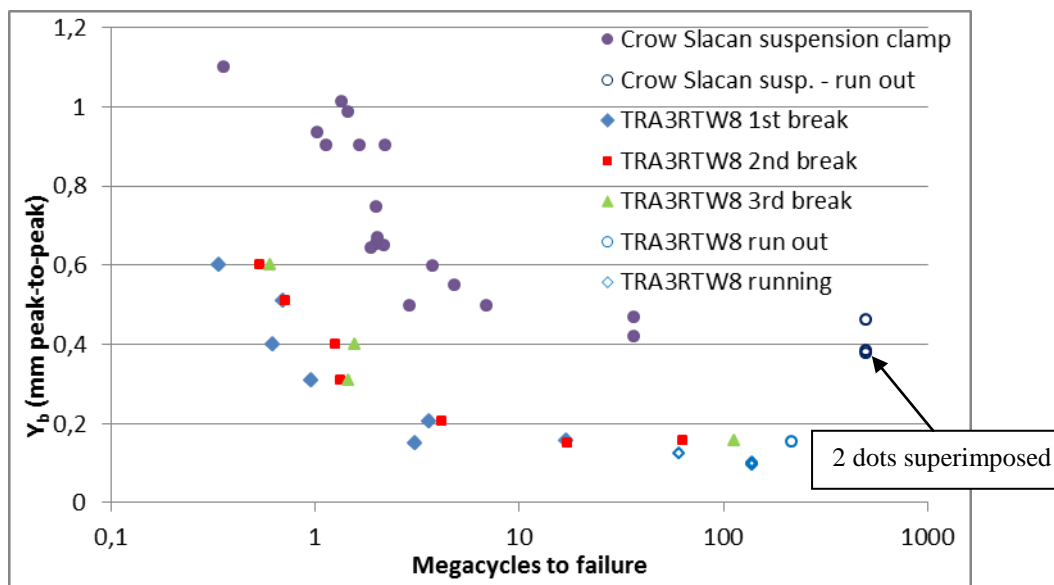


**Figure 11: Comparison of the number of cycles before breaking for the TRA3RTW8 and a Crow conductor in a metal-to-metal clamp as a function of  $Y_b$**

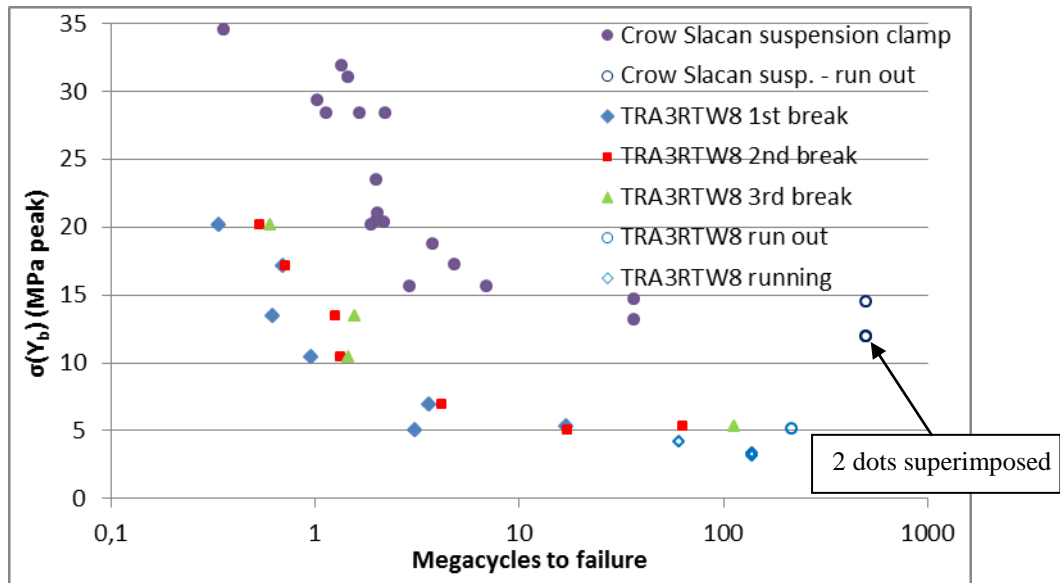


**Figure 12: Comparison of the number of cycles before breaking for the TRA3RTW8 and a Crow conductor in a metal-to-metal clamp as a function of  $\sigma_a(Y_b)$**

### VALIDATION OF THE DAMPING SYSTEM

The damping system will be validated during fall 2019. The TRA3RTW8 conductor with all anchor hardware, including the dead-end joint at the end of the river crossing, will be installed on a 63.5-m laboratory span (Figure 14). The relative displacement of the conductor will be measured at the outlet of the dead-end joint and the reverse relative displacement at the damper clamps to ensure that the dampers dissipate sufficient energy for the vibration amplitudes to remain below the limit of endurance. The dissipated power will be measured by the power technique and will be compared to the wind power injection calculated with the equation provided in IEC 61897 [1998].



**Figure 13: Crow conductor and metal-to-metal suspension clamp (Slacan 62065)**



**Figure 14: Laboratory span of 63.5m**

Aeolian vibration dampers with preformed rod attachments rather than bolted clamps will be used to maximize the conductor's tolerance to vibration in the damper clamp and prevent problems of bolts loosening and the damper slipping along the conductor. A slip test of the preformed rod attachment on the conductor has been performed to ensure that the damper will be properly restrained on the conductor and will not migrate to the low point of the span over time.

## CONCLUSION

The paper presents fatigue test results for one type of conductor for which no data is available, namely an ACSR conductor, for a St. Lawrence River crossing that combines the following characteristics:

- Conductor's envelope made of aluminum alloy
- Conductor's envelope made of trapezoidal wires
- Conductor retained by a dead-end joint on each side of each suspension tower rather than being supported in a suspension clamp
- Very high conductor's H/w setting of 6350 m.

Based on eight fatigue tests carried out at relative displacements  $Y_b$  of 0.15 to 0.6 mm peak-to-peak, it is clear that the endurance limit of the conductor TRA3RTW8 in dead-end joint will be much lower than that of an ACSR in a standard metal-metal clamp. Additional tests are in progress at amplitudes of 0.100 and 0.125 mm peak-to-peak.

For a given mode of vibration, the relative displacement  $Y_b$  is directly proportional to  $fY_{\max}$ , as shown for amplitudes of 50, 100 and 150 mm/s in mode 6 for two different tests.

For the same  $fY_{\max}$  at the vibration antinode, the relative displacement  $Y_b$  of the conductor at the outlet of the dead-end joint is at its maximum when the outlet of the dead-end joint is close to the vibration antinode. It will therefore be necessary to ensure that the chosen damping system adequately protects the conductor over the entire range of frequencies of interest and in particular at frequencies for which the end of the joint is close to the vibration antinode.

## BIBLIOGRAPHY

CIGRE (2005). *Overhead conductor safe design tension with respect to aeolian vibrations*. Technical brochure CIGRE 273, 43 pages.

IEC 61897 First edition (1998). *Overhead lines – Requirements and tests for Stockbridge type Aeolian vibration dampers*, 54 pages.

CEI 62568 Edition 1.0 (2015). *Overhead lines – Method for fatigue testing of conductors*, 38 pages.

EPRI (2009). *Transmission line reference book: Wind-induced conductor motion*, Second edition. Electric power research institute (EPRI), Palo Alto, CA.

GREMCA (August 2002) Université Laval, Essais de fatigue du conducteur ACSR Crow avec amplitude variant selon une distribution de Rayleigh, Rapport No. SM-2002-07, Québec, Canada.

J. Paradis, P. Van Dyke (2019) *Improved conductor endurance limit by using a suspension clamp with conical elastomers*, CIGRE Canada 2019, Montréal, Québec, Canada, 8 pages.